https://doi.org/10.1016/j.jenvman.2021.113359

A machine learning approach for prioritizing groundwater testing for per-and polyfluoroalkyl substances (PFAS)

Sarabeth George[a,*], Atray Dixit[b]

[a]California State Water Resources Control Board; sarabethgeorge@gmail.com

[b]Coral Genomics, San Francisco, CA 94107, USA; atray@coralgenomics.com

*Corresponding author

Abstract

Regulatory agencies are beginning to recognize and regulate per-and polyfluoroalkyl substances (PFAS) as concerning environmental contaminants. In groundwater management, testing and mitigation strategies are desirable, but can be time and cost-intensive processes. As a result, only a fraction of all groundwater wells has been tested for PFAS levels, resulting in potentially extended drinking water exposure to PFAS in the meantime. In this study, we build a series of machine learning models (including linear and random forest regressors) to predict PFAS based on a groundwater dataset from California. These models are used to compare the relative predictive ability of co-contaminant fingerprints, hydrological properties, soil parameters, proximity of airports/military bases, and geospatial data. Additionally, a random forest machine learning model that combines all data types can quantitatively predict the maximum PFAS compound concentration in a well with a Spearman correlation of 0.64 and can discern wells containing concerningly high concentrations of PFAS with an accuracy of 91% (AUC of 0.90). This approach may have widespread utility for other hazardous anthropogenic compounds in groundwater. Future investigations should evaluate the practicability of using machine learning to prospectively prioritize contaminant testing in groundwater wells.

Introduction:

Per-and poly- fluoroalkyl substances (PFAS) are a class of water-soluble anthropogenic contaminants of increasing global concern due to their ubiquity in the global environment, persistence, and toxicity. Management of PFAS contamination in water resources requires cross-cutting approaches in multiple industries, from management of solid and liquid wastes to monitoring and regulation of industrial operations and drinking water. PFAS have been used extensively in many products including textile coatings, surfactants, pesticides, food contact materials, and fire-fighting foams since the mid-20th century (Prevedouros et al., 2006; Wang et al., 2017). The primary source of PFAS to the environment is estimated to be industrial emissions (Prevedouros et al., 2006), however, PFAS are also known to be formed as the result of breakdown of "precursor" compounds such as fluorotelomer alcohols and perfluoroalkyl sulfonamido alcohols (Fasano et al., 2006; Martin et al., 2006, 2005). Many studies have shown that PFAS compounds persist in the environment, bioaccumulate, and are toxic (Conder et al., 2008; De Silva et al., 2021; Frömel and Knepper, 2010; Houtz et al., 2013; Parsons et al., 2008; Young and Mabury, 2010). PFAS have been detected throughout the global environment, biota, and humans; the 2011–2012 United States National Health and Nutrition Examination Survey found detectable PFAS in 97% of individuals tested (Giesy and Kannan, 2001; Lewis et al., 2015; Rayne and Forest, 2009; Vestergren and Cousins, 2009). Studies have linked several PFAS, including perfluorooctanonate (PFOA) and perfluorooctane sulfonate (PFOS), with adverse effects on environmental and human health, including decreased birth weight and increased incidence of liver, pancreas and testicular tumors (Biege et al., 2001). The primary pathways of human exposure to PFAS is include diet, indoor environments polluted with PFAS, and PFAS-contaminated drinking water (Domingo and Nadal, 2019; Sjogren et al., 2016; Vestergren and Cousins, 2009). Blood serum PFAS in humans

has been shown to be positively related to drinking water PFAS concentration (Ericson et al., 2008; Kannan et al., 2004; Xu et al., 2020).

In California, the geographic focus of this study, approximately 40% of drinking water is supplied by groundwater wells. In drought years, up to 60% of drinking water is sourced from groundwater (Carle, 2015). PFAS has been detected in California in both the influent and effluent of wastewater treatment plants (Houtz et al., 2018); in urban stormwater runoff (Houtz and Sedlak, 2012; Plumlee et al., 2008); in urban rivers (Plumlee et al., 2011; Sengupta et al., 2014); and in the tissues of marine mussels (Dodder et al., 2014). Between 2013-2015, six PFAS contaminants were systematically sampled in drinking water in the United States for the first time as part of the United States Environmental Protection Agency (USEPA) Third Unregulated Monitoring Rule, or UCMR3 Report; this study showed widespread PFAS contamination at concerning concentrations in water samples nationwide, including detections in California (Crone et al., 2019; Hu et al., 2016; US EPA, 2015). Furthermore, recent studies have found significant correlations between drinking water PFAS concentration and sera concentrations of PFAS in Northern California (Hurley et al., 2016; Kim et al., 2020). In response to growing concerns and public pressure regarding PFAS contamination in California, the California State Water Resources Control Board (State Water Board) began issuing investigative orders in 2019, targeting high-risk drinking water systems and known potential source sites (State Water Resources Control Board, 2020). Results of these analyses have been publicly shared on the Groundwater Ambient Monitoring and Assessment (GAMA) database.

Both in the State of California, and globally, current frameworks for prioritizing drinking water testing for PFAS are poorly suited to identifying contamination in areas not directly adjacent to known source industries and facilities; furthermore, representative sampling of the more than one

million groundwater wells in California, particularly private wells, will take years. This study presents a novel method for risk assessment of PFAS contamination using co-contaminant fingerprints, airport and military installation proximity, hydrological, soil and geospatial data as features to train a machine learning model. The hypotheses driving this investigation are (1) that anthropogenic contaminants, including PFAS, follow consistent patterns in the environment both in terms of patterns of release from source areas and transport/transformation over time (Alimi et al., 2003; Barrett et al., 1999; Douglas et al., 2007; Kibbey et al., 2020; Le et al., 2021) and (2) these consistent patterns can be leveraged to predict the risk that PFAS will exceed regulatory thresholds using supervised machine learning. In the future, predictions from supervised machine learning applications could be used to prioritize sampling of the highest-risk drinking water wells, reducing human exposure to unsafe concentrations of PFAS.

Materials and Methods

Generation and curation of dataset

Data was downloaded from the Geotracker Groundwater Ambient Monitoring and Assessment (GAMA) database (California State Water Resources Control Board, 2020). The GAMA Program is California's comprehensive groundwater quality monitoring program that was created by the State Water Board in 2000. It was later expanded by Assembly Bill 599–the Groundwater Quality Monitoring Act of 2001–requiring the State Water Board to assess groundwater quality in basins that account for 95% of the state's groundwater use. This system provides access to approximately 87 million analytical results from over 290,000 wells in California for more than 200 analytes, spanning the 1960's to present. Notably, given the fact that PFAS in groundwater has been linked use of fire-fighting foams at military bases in the United States, military

installation groundwater monitoring data is generally not available in GAMA, including recent US Department of Defense studies on PFAS (Hu et al., 2016).

For this study, the dataset was filtered based on duplicate wells and wells that had fewer than 5 analyte measurements to a set of 189,972 wells across 228 analytes (approximately 4.7% of the values of this dataset are not missing); for wells where analyte data was available for multiple sampling events, the average value was used. The chemical data for each well was normalized using a log10(analyte in parts per trillion (ppt)+1) transformation. It was then combined with geospatial data including latitude, longitude, and other metadata. The summary statistics for the maximum PFAS concentration for each well is summarized in **Table 1** below and for the broader set of co-contaminants in **Table S1**.

Other datasets included: the number of nearby (within 1.5 mile radius) airports/military bases, depth to groundwater, elevation, 15 soil hydraulic properties, and 15 features representing other soil properties. These data types (and their sources) are summarized in **Table 2**.

Table 1: Summary of PFAS measurements in dataset. Values are based on a $\log_{10}$(PFAS compound in ppt+1) scale.

	# of wells	**mean**	**std**	**min**	**max**
Maximum PFAS value per well	1410	1.30	0.77	0.01	5.0

Table 2: Summary of the various feature categories/subsets used in the machine learning model to predict PFAS.

Feature (name used in paper, if different)	**Number of features**	**Description**	**Source**
Nearby airports and military bases (airport/military base proximity)	9	The number of nearby large, medium, or small airports, seaplane bases, heliports and whether they are active or closed. AND The number of nearby large, medium, or small military bases and whether they are active or closed.	https://ourairports.com/data/ https://public.opendatasoft.com/explore/dataset/military-bases
Geospatial	3	Latitude, longitude, and elevation	("Elevation Point Query Service," n.d.; State Water Resources Control Board, 2020)
Hydrology and soil hydraulic properties (Hydrology)	15	Depth to groundwater Means and standard deviations associated with field capacity, h_m, K_s, Plant available water, Sigma, θ_r, θ_s	California Natural Resources Agency, n.d. and Zhang et al., 2018
Soil	15	Terrain, land cover, soil quality	Fischer et al., 2008
Co-contaminants	228	Groundwater quality data for over 290,000 wells in California	(State Water Resources Control Board, 2020)

Linear Model

Linear regression is a simple machine learning method that can be used to solve for the best fit line relating each of a set of features to a target variable of interest. In this paper we use it as a benchmark to compare performance against nonlinear models (such as Random Forest Regression, described below). We use the *sklearn.linear_model.Ridge* method from Python

which applies a penalty term for slopes (coefficients) that have a large magnitude in order to reduce the likelihood of overfitting.

Random Forest Regression

Random forest regression is an ensemble method that uses a collection of decision trees to derive estimations of the likely value of a target variable given a set of features. When using a Random Forest Regressor, the *sklearn.ensemble.RandomForestRegressor* method in Python was used. The number of estimators was set to 1000 and the *min_samples_leaf* was set to 2. The performance of the Random Forest Regressor was evaluated based on cross-validation described below.

Cross-validation: random and geospatially localized grouping

In order to evaluate the performance of our machine learning approach to predict PFAS levels, wells were grouped into 10 equal sized subcomponents. We created these groups using two separate methods. In the first, groundwater wells were randomly assigned to each of 10 groups (map in **Figure 3A**). In the second, data was split using a modified version of k-nearest neighbors clustering such that each group contained wells from a unique geospatial region. (**Figure 3B**).

For each of these approaches, cross-validation was performed with nine of the groups used for training the machine learning model and the last group used as a test set to evaluate the model's performance (on data the model had not been trained on). This cross validation was repeated until each group had been used as the test set.

Step by step procedure of model training, evaluation, and application

1. Collate the feature subsets (airport/military base proximity, geospatial data, soil properties, hydrologic properties, co-contaminants), and a combined feature set with all of the subsets for all wells with the analyte of interest (in the case of PFAS, 1,410 wells).
2. Mask the analyte of interest from feature sets containing co-contaminant data (in the case of predicting the maximum PFAS value, all chemicals in the PFAS class were masked).
3. Divide the data into 10 groups using geospatial clustering or geospatially random cross validation approach described in *Cross-validation* above.
4. Train separate linear model and random forest regressors (as described above) to predict the analyte of interest trained on nine out of the 10 groups using each of the feature subset as well as the combined feature set.
5. Capture the predicted value on the hold out group as well as the Spearman correlation between the actual and predicted value.
6. Repeat across all groups.
7. Determine the best performing model.
8. Apply best-performing model to predict analyte levels of wells that have not been tested.

Derivation of confidence interval estimates from Random Forest Regressor

In order to create estimates of the robustness of the machine learning model predictions, we leveraged the bagged nature of the Random Forest model (in which the estimates associated with many decision trees are averaged) to derive an estimate of the variance in the prediction across all trees (Wager et al., 2014). This method is implemented in the *forestsci* package in python.

Visualization of PFAS values and predictions on maps

The plotly express package in python was used to plot and visualize PFAS values on a map of California.

Results:

We sought to leverage the public datasets available through the California GAMA system as described in **Methods**, to build a machine learning approach that could predict groundwater wells with the greatest risk for high PFAS concentration (**Figure 1**). The machine learning model predicts known PFAS measurements given other chemical measurements (i.e. potential co-contaminants of PFAS), airports/military base proximity, depth to groundwater, soil hydraulic properties, soil properties, (**Supplementary Table 1**) and geospatial data (elevation, latitude, and longitude). This machine learning model can be applied to wells in which PFAS levels have not been measured in order to predict PFAS concentration at that location (**Figure 1C, D**).

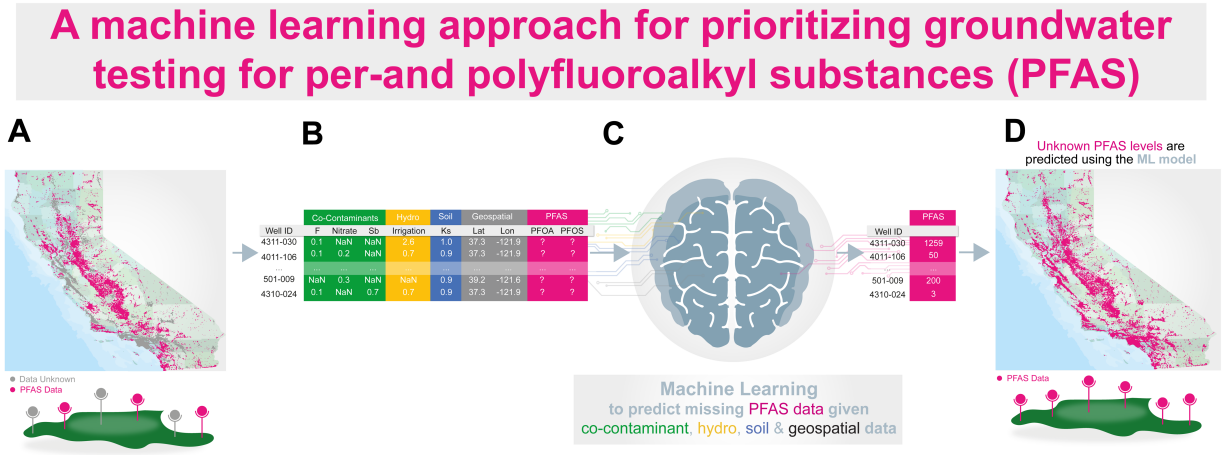

Figure 1. An overview of a machine learning approach to enable proactive water resource management for PFAS

(**a**) Visualization of the location of each of the 189,972 groundwater wells in the State of California that were used as part of this study (**b**) Visualization of the chemical co-contaminant

data types (green), hydrological data (yellow), soil data (blue), geospatial data (gray), and PFAS measurements (pink) used in this study; airport/military base proximity data is not included in this figure for simplicity. Columns correspond to different measurements and rows correspond to different wells. "NaN" indicates to missing feature data and question mark symbols indicate missing PFAS data that the machine learning model seeks to predict. (**c**) A machine learning approach is used to predict PFAS data (pink) given the other data types. (**d**) This machine learning model can then be applied to predict unknown PFAS levels in wells with no PFAS testing performed, which can be in turn used to prioritize testing.

A diverse set of features used as inputs to a machine learning model trained on existing PFAS data

PFAS measurements in our curated dataset were distributed throughout the State of California (**Figure 2A**). We sought to incorporate diverse data types that may potentially be predictive of PFAS levels (see **Table 2**, **Figure 2B, C**). A particular challenge in this co-contaminant data, and in other similar monitoring datasets, is that very few wells have been tested across every possible analyte. In the entire dataset, only 4.7% of chemical measurements across all possible analytes and all possible wells have been tested. A naïve solution to handling this level of missing data would be to focus on a subset of analytes and wells in which the data is relatively complete. However, this would discard a tremendous resource associated with rich co-contaminant correlation structure in this dataset (**Figure 2C** and **Supplementary Figure S1**). There are many non-PFAS analytes/features with strong associations with PFAS compounds such as a strong positive relationship between TBA (Tertiary butyl alcohol) and PFOA and a weak negative relationship between PFUNDCA (perfluoroundecanoic acid) and SC (specific

conductance) (**Figure 2C**). Such correlations form the basis on which a machine learning model can predict unmeasured contaminants in the absence of their direct measurement.

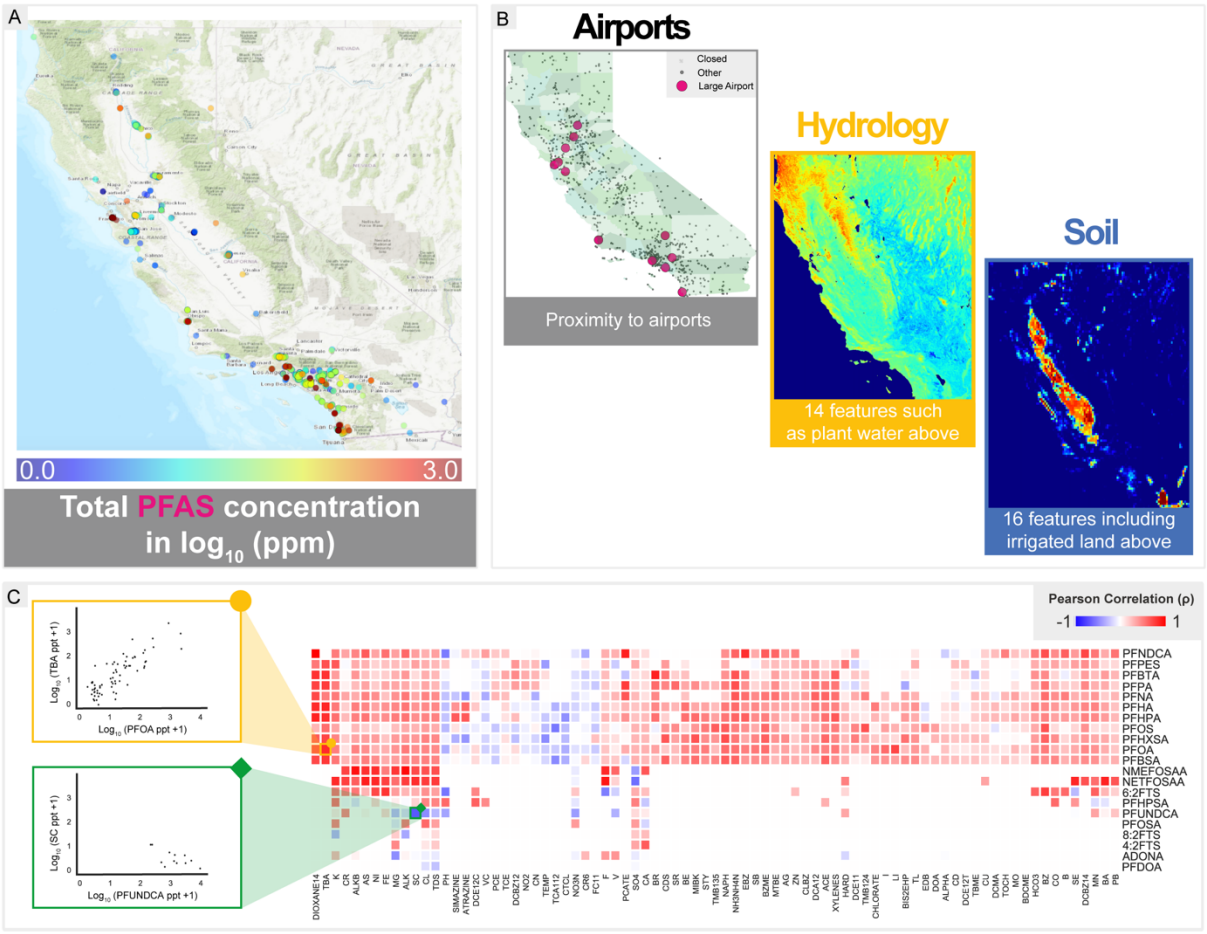

Figure 2. A diverse set of features used as inputs to a machine learning model trained on existing PFAS data.

(**a**) Visualization of the location of each of the 1,410 groundwater wells (dots) in the State of California that had associated PFAS measurements in our dataset. Each well is colored by total PFAS concentration on a log10 scale. (**b**) Geospatial visualization of different feature types from left to right: airports in California with larger pink dots corresponding to large airports, hydrology and hydraulic soil properties, and soil properties. (**c**) A correlation matrix visualization of pairwise

correlations between PFAS compounds with non-PFAS co-contaminants. Each cell represents the Pearson correlation between the respective elements as shown in the yellow and green scatter plots. The color scale ranges from red to blue, corresponding to a correlation between 1.0 and -1.0.

Different machine learning models to evaluate importance of feature subsets and nonlinearities

We created several machine learning models to predict the maximum PFAS value for a given well. Separate models were developed using each of the feature categories in order to provide an estimate of their relative predictive power as well as a combined model across all features. For each of these cases, we evaluated the performance of a regularized linear regression in comparison to a random forest model using two forms of cross validation (see **Methods**). By comparing the results from a cross validation in which wells were randomly grouped, to a cross validation performed on wells geospatially separated from wells used for training, we were able to understand the extent to which the model's predictions are highly dependent on local regional variation. By comparing the results from a linear model to those of a random forest, we were able to understand the relative importance of nonlinear interactions between features for the prediction task.

Machine learning model accurately predicts individual PFAS compounds and overall PFAS abundances

We find that for cross-validation in which wells are geospatially randomized, each feature subset can be used independently to predict PFAS. Spearman correlations between predicted and actual maximum PFAS value ranged from 0.19 for the airport proximity model ($p<10^{-4}$) to 0.64 for the combined model ($p<10^{-9}$). Additionally, for all feature subsets except the number of nearby airports, a random forest regression significantly outperformed the linear model (p-values 0.58,

230 $1.4x10^{-12}$,$1.4\ x10^{-8}$, $4.4x10^{-7}$, $2x10^{-4}$ for airport, geospatial, hydrological, soil, and co-
231 contaminants respectively). Finally, a combined model across all features outperformed any of
232 the individual feature subsets (**Figure 3A**). We demonstrate strong correlation of the predictions
233 of this combined model with the actual measured maximum PFAS level along with uncertainty
234 estimates in the model predictions (**Figure 3C**). For cross-validation in which wells are
235 geospatially clustered, co-contaminant features were the most reliably predictive ($p<5x10^{-5}$). A
236 combined model across all features did not outperform the co-contaminant alone model ($p=0.98$).
237 (**Figure 3B**)

238 We then applied the results of our ML approach to all wells in the GAMA dataset that have not
239 yet been tested. This resulted in a nearly 130-fold increase in the number of wells with PFAS
240 estimates as well as the identification of a sizable number of wells with concerningly high
241 predicted PFAS levels (**Figure 3D**). We assessed the extent to which wells where PFAS has been
242 measured (our training / testing data) differ significantly from wells that have not been measured
243 for PFAS with respect to their co-contaminant profile. While the wells do not differ drastically
244 from other wells with respect to co-contaminant profiles (see dimensionality reduction
245 visualization in **Figure S3A**), we note that wells that have had PFAS levels measured have
246 significantly had more co-contaminant measurements performed on them than wells that have
247 not had PFAS measured (**Figure S3B**).

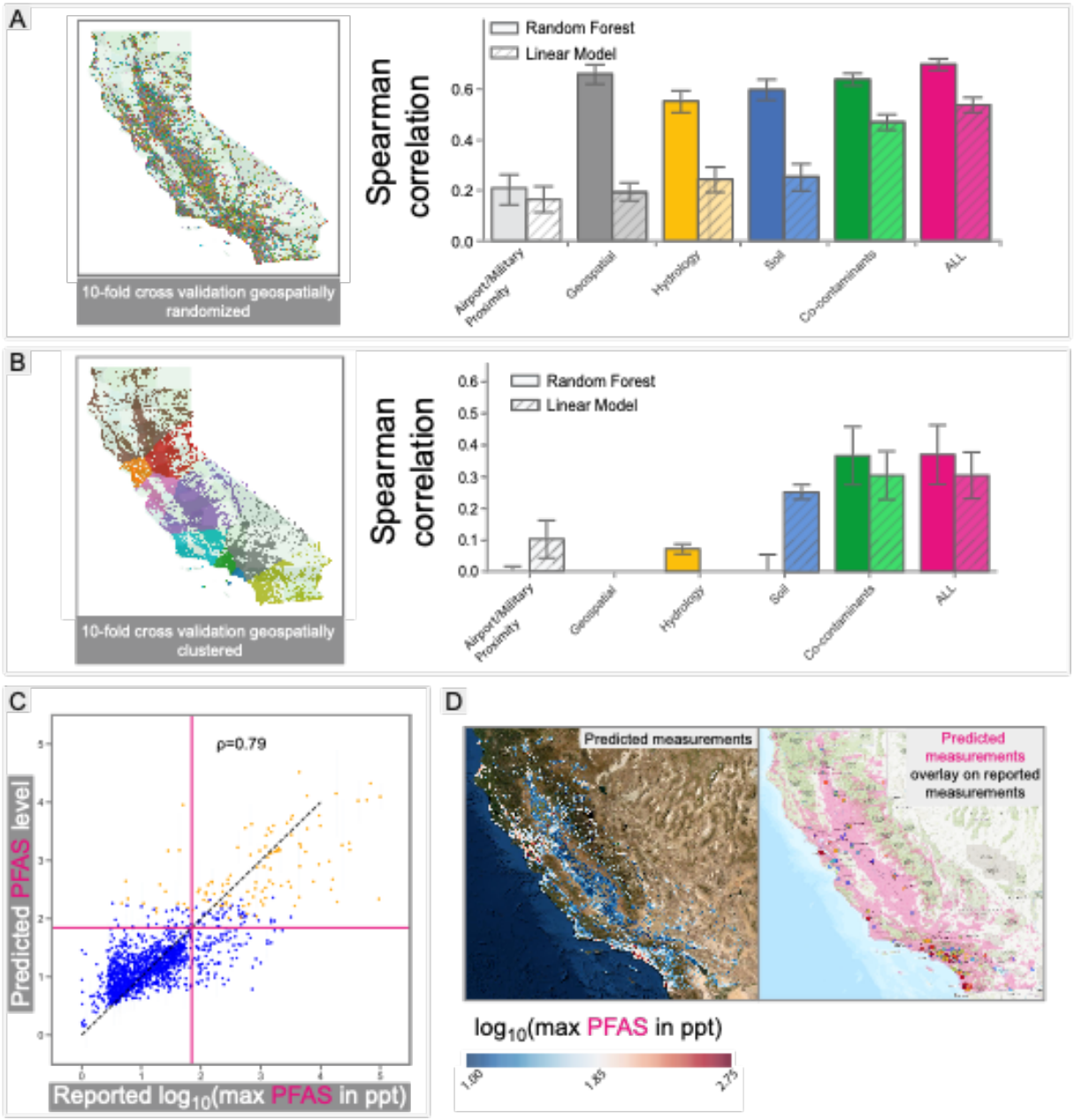

Figure 3. Machine learning model accurately predicts individual PFAS compounds and overall PFAS abundances

(**a**) Results from models evaluated using a geospatially randomized cross validation. Wells were assigned randomly to one of 10 categories as shown on the map on the left (colors correspond to

various categories). Bar plots for model performance across each of the 10-folds on right for each of the feature subsets and combined model. Y-axis corresponds to Spearman correlation between predicted and actual maximum PFAS level (log_{10} ppt) across wells in test set. Error bars represent 95% confidence intervals. (**b**) Results from models evaluated using a geospatially clustered cross validation. Wells were assigned to one of 10 categories based on geospatial locations as shown on the map on the left (colors correspond to various categories). Bar plots for model performance across each of the 10-folds on right for each of the feature subsets and combined model. Y-axis corresponds to Spearman correlation between predicted and actual maximum PFAS level (log_{10} ppt) across wells in test set. Error bars represent 95% confidence intervals. (**c**) Scatter plot between reported maximum PFAS level (x-axis, log_{10} ppt) and predicted maximum PFAS level (y-axis). Error bars correspond to two standard deviations of model predictions. Horizontal and vertical lines correspond to 70 ppt. Orange dots correspond to wells whose lower bound on predicted maximum PFAS level is above 70 ppt. (**d**) Map of predicted PFAS levels across all 189,972 groundwater wells.

Practical advantage of a risk adjusted testing strategy based on a machine learning model.

Lastly, we sought to quantify the model's performance when applied to a specific regulatory threshold. We quantified its performance when identifying wells that have a maximum PFAS concentration greater than 70 ppt, equivalent to the current USEPA Health Advisory Level for the sum of PFOA and PFOS. The 70 ppt threshold was chosen as a benchmark measure for wells that may present elevated risk, although our analysis includes additional PFAS besides PFOA and PFAS. At a 5% false positive rate, the model recovered 67% of the true positive results in an overall area under the curve of 0.90 (**Figure 4A**). To demonstrate how this model would be used in a real world context, we simulated how quickly all wells with maximum PFAS levels greater

than 70 ppt would be discovered using various strategies. We compare a strategy in which the wells with the highest machine learning predicted PFAS levels were tested first with either a random guessing strategy or a strategy in which the wells are guessed perfectly (**Figure 4B**). The machine learning-informed strategy significantly outperformed a random sampling approach ($p<10^{-7}$).

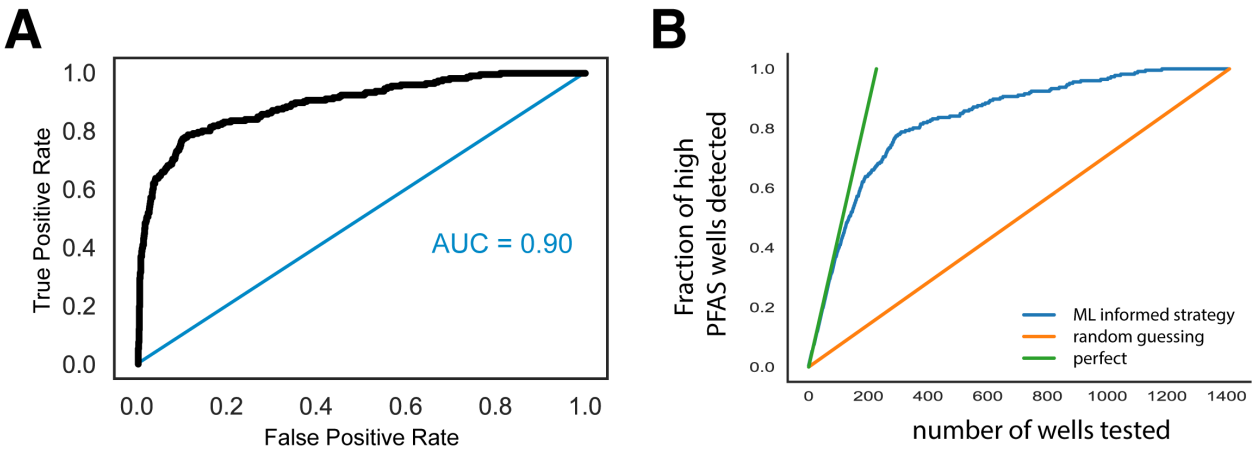

Figure 4. Practical advantage of a risk adjusted testing strategy based on a machine learning model.

(**a**) Receiver operating characteristic curve demonstrating model performance for predicting wells where the maximum PFAS exceeds 70 ppt. Blue diagonal line represents the expected model performance for a model which guesses randomly based on the average likelihood of a well exceeding the threshold. (**b**) Results of a machine learning-informed testing strategy in which wells with a predicted maximum PFAS level greater than 70 ppt are tested first (blue line). This result is compared to a strategy in which wells are tested randomly (orange line) and one in which wells with maximum PFAS level greater than 70 ppt are predicted perfectly (green line).

Discussion:

Co-occurrence of chemical analytes in drinking water can be used for accurate machine learning approaches for PFAS

A machine learning model based on co-contaminant data alone was able to significantly predict maximum groundwater PFAS concentration regardless of whether or not it was trained on wells in a similar geographic area to those upon which its performance was evaluated. Co-contaminant data may act as a proxy for water management practices like water recycling and wastewater injection in features such as ions (Ca^{2+}, Mg^{2+}, Na^{+}) and parameters including specific conductivity. Land use practices are likely also reflected in co-contaminant data: various regional industries drive requirements to monitor groundwater for different contaminants regionally (e.g., pesticides in agricultural areas and chlorinated solvents in industrial areas). The addition of airport/military base proximity, geospatial data, soil properties, and hydrologic properties boost model performance, but only when the wells used for evaluating performance geographically overlap with those used for training the model.

Generalization across other contaminants and geographies

Our results indicate that predictions using co-contaminant features are more generalizable across contaminants and geographies than predictions using more locally specific features such as geospatial, hydrologic and soil parameters. In geospatially randomized cross-validation trials, each feature set (co-contaminants of PFAS, nearby airports, soil hydraulic properties and geospatial data) can be used independently to predict PFAS, however, in geospatially clustered

cross-validation trials, predictive power across all features was reduced. This pattern is generally conserved across the 228 analytes in our dataset, notably, for many analytes for which the total number of measurements exceeds that available for PFAS by >10 fold, e.g. 1,1-Dichloroethene (DCE11) (**Figure S3B**). Overall, models to predict PFAS perform best when trained on wells in geographically similar areas to those it is ultimately used to predict unknown values.

Recommendations to stakeholders

In the United States, State governments are beginning to make historical groundwater (and other environmental) monitoring data available to the public, but the potential of these data resources has thus far been underappreciated. Generally, the performance of machine learning methods such as those outlined in this paper improve with the amount of data available; indeed, we observed significant correlation between the size of the training dataset and model accuracy when we applied our integrated machine learning model approach to each of the 228 analytes in the dataset, $p<10^{-9}$, **Figure S3**). We have demonstrated the potential of aggregating groundwater contaminant measurements despite a significant level of sparsity with a high degree of missing data elements (in this case excess of >95% missing). This result highlights the need for collaborations between regulatory bodies across state and national boundaries to bring together environmental datasets in an open-source data framework. In such a framework, machine learning methods such as these may be able to more rapidly identify and mitigate the most dangerous sources of anthropogenic groundwater contamination. In order for the GAMA dataset, and other similar public datasets to reach their full potential to support protection of human health and the environment, cooperation between both regional and Federal governments is imperative. For example, in the GAMA dataset, a significant shortcoming is that results from

338 military bases are generally absent, because results from Department of Defense (DOD) cleanup
339 projects are not uploaded to the GAMA database; since DOD installations are a known source of
340 PFAS, this is a significant blind spot.
341 Application of computational techniques on existing monitoring datasets is a promising method
342 for improving detection of groundwater wells which pose a threat to human health. This
343 technique may even reveal previously unknown areas of concern for well-characterized
344 contaminants in addition to its utility in investigating emerging contaminants like PFAS. As
345 more regional and Federal governments make these data available, it will become possible to
346 create massive datasets of high-resolution historical groundwater data for many contaminants,
347 which may aid in scientific understanding of patterns of release and transport. Better
348 understanding of release and transport of contaminants that pose a threat to public health will
349 support proactive management and protection of groundwater resources, both by enabling
350 regulation of facilities and industries found to discharge contaminants of concern, and by
351 optimizing pumping, treatment and blending of extracted groundwater used as drinking water to
352 protect human health.

353 Machine learning tools such as those described in this study have the potential to aid in better
354 mitigation of the cumulative environmental contamination burden in high-risk communities by
355 providing robust integrated predictions of exposure to contaminant classes such as PFAS. We
356 recommend that these tools be used to implement additional testing of the highest-predicted-risk
357 wells rather than as a method for determining entire monitoring schedules. This is because with
358 the application of any computational method that makes predictions on historical data, inherent
359 biases in the data (e.g., exclusion of DOD data) are a significant concern when evaluating and
360 applying predictions, especially when predictions can affect public health. In particular, we

emphasize the potential environmental justice pitfalls of relying naïvely on machine learning predictions to make regulatory decisions. In the United States, heavy-polluting industries and facilities have historically been built in or adjacent to socioeconomically and racially segregated neighborhoods due to a combined history of exclusionary residential real estate practices and zoning laws (Maantay, 2002; Mohai et al., 2009; Mohai and Saha, 2015). These invisible sociohistorical overprints on the groundwater monitoring data are not unique to the United States and will need to be investigated further as a central aspect of integrating machine learning and other big-data approaches into water management and regulation.

A future scientific challenge remains to tie individual chemical dose-effects to multi-chemical integrated hazard indices for human and environmental health; key to this is understanding how multiple chemical exposures interact to produce cumulative health effects. Such efforts should drive the determination of regulatory limits that machine learning frameworks, such as the one described here, can be optimized towards.

Conclusions:

Contaminants in drinking water pose a significant threat to human health. With limited resources and a growing number of emerging contaminants, direct testing of all possible contaminants is infeasible. In this study, we develop a machine learning framework that can be used to prioritize groundwater wells for testing using the limited resourced available. The machine learning framework leverages diverse geospatial and chemical co-contaminant measurements to accurately predict contaminants such as PFAS. Despite the high levels of missing data in the co-contaminant data (in which only a small portion of the total possible measurements are available for a given well), we demonstrate that there is sufficient structure to create accurate predictive models. We found that co-contaminant features can be robustly predictive of unseen analytes,

including PFAS, even when the machine learning model is trained on wells geographically distinct from those it is applied to.

This result suggests our model for predicting PFAS has the potential to significantly accelerate the ability to identify groundwater sources with concerningly high PFAS concentrations. Strikingly, our model is projected to reduce the number of wells required to detect 70% of concerningly high PFAS wells by a factor of five compared to a random sampling approach. In general, we believe our approach could have broad utility in aiding regulatory agencies in overseeing the management of anthropogenic contaminants in groundwater using predictive analytics to guide testing strategies.

Acknowledgements

The authors thank Erica Kalve for offering support, encouragement, and expertise, as well as colleagues at the San Francisco Bay Regional- and State of California- Water Resources Control Boards for fruitful discussions of groundwater contamination and emerging contaminants; in particular, the 2019 PFAS Summit and Datathon team. We would also like to thank Ari Frizzle for moral support.

Declaration of competing interest

A.D. is a founder of and equity holder in Coral Genomics. The authors alone are responsible for the views expressed in this publication and they do not necessarily represent the views, decisions or policies of the institutions with which they are affiliated.

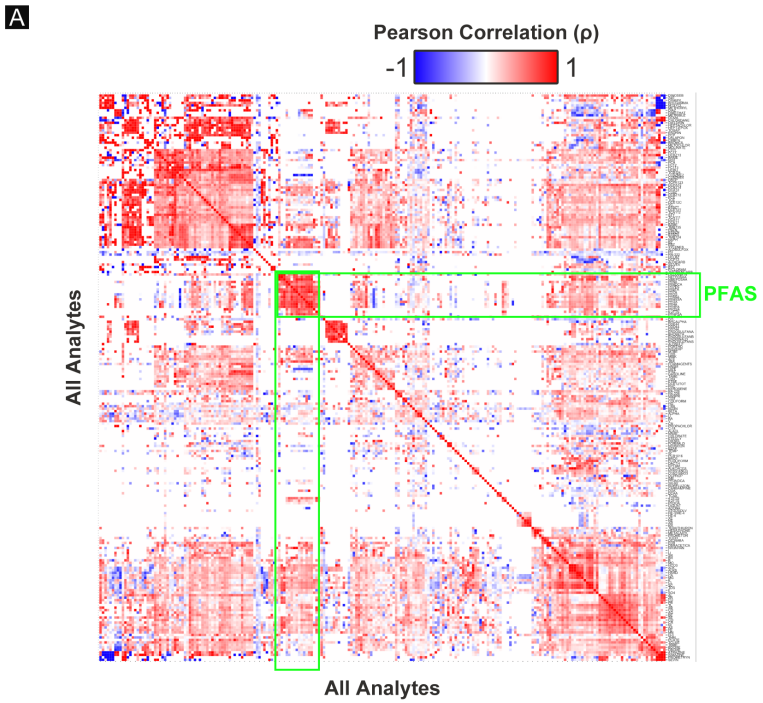

Figure S1. An overview of pairwise correlations between chemical and geospatial features in the GAMA dataset.

A correlation matrix visualization of pairwise correlations between chemical and geospatial features. Each cell represents the Pearson correlation between the respective elements as shown in the yellow and purple scatter plots. The color scale ranges from red to blue, corresponding to a correlation between 1.0 and -1.0. The PFAS set of compounds is highlighted in green (this region overlaps with the data displayed in **Figure 2C**).

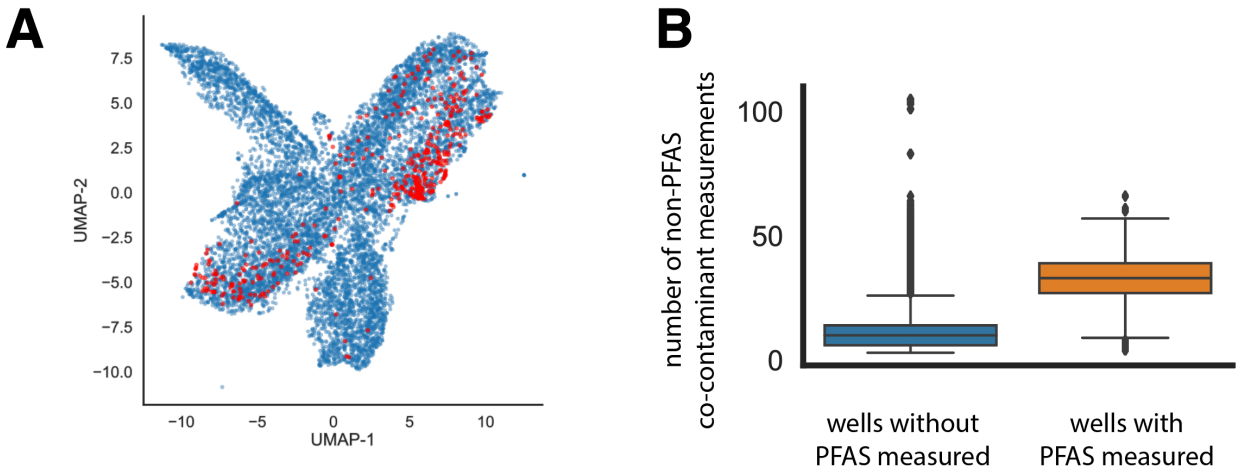

412

413 **Figure S2. Comparison between wells that have had PFAS measured and those that have not**

414 (**a**) After performing PCA on the co-contaminates dataset across all wells, dimensionality

415 reduction was performed using UMAP. Wells that have had PFAS measurements are highlighted

416 in red. (**b**) Boxplot showing the difference in the number of analytes measured in wells that have

417 had a PFAS measurement compared to those that have not had a PFAS measurement. Boxplots

418 denoting interquartile range, 1.5 times this distribution with whiskers, and outliers as dots.

419

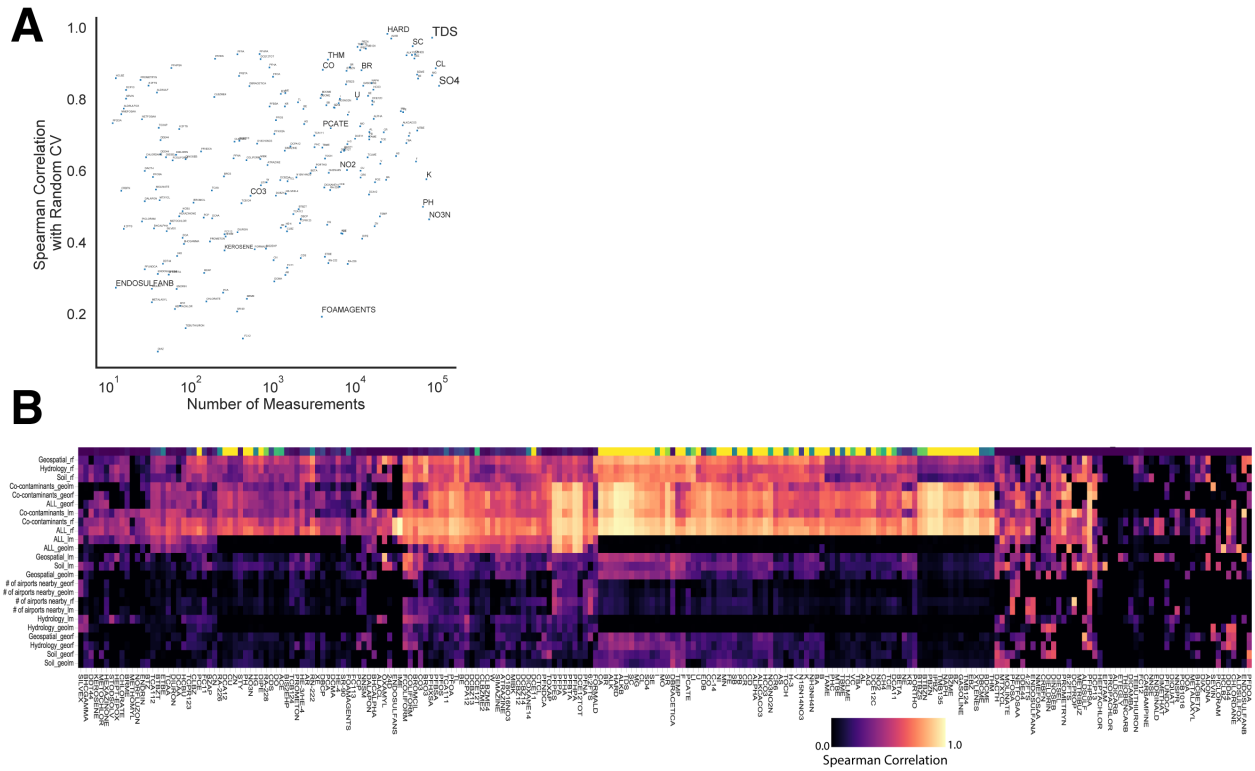

Figure S3. Results of application of model to all 228 chemicals.

(**a**) Scatter plot of the number of measurements on a log10 scale (x-axis) vs. the average Spearman correlation of the test set performance across all 10 folds for a machine learning model trained to predict that chemical analyte.

(**b**) Spearman correlation of the different model types (rows) applied to predicting each of the 228 chemical analytes (columns). Georf = geospatially clustered cross validation random forest. Geolm = geospatially clustered linear model. lm = linear model. rf = random forest. First row is an a colorimetric representation of the number of total measurements there were available for the corresponding analyte in the dataset.

References:

433 Alimi, H., Ertel, T., Schug, B., 2003. Fingerprinting of hydrocarbon fuel contaminants:
434 Literature review. Environ. Forensics. https://doi.org/10.1080/15275920303489

435 Barrett, M.H., Hiscock, K.M., Pedley, S., Lerner, D.N., Tellam, J.H., French, M.J., 1999. Marker
436 species for identifying urban groundwater recharge sources: A review and case study in
437 Nottingham, UK. Water Res. https://doi.org/10.1016/S0043-1354(99)00021-4

438 Biege, L.B., Hurtt, M.E., Frame, S.R., O'Connor, J.C., Cook, J.C., 2001. Mechanisms of
439 extrahepatic tumor induction by peroxisome proliferators in male CD rats. Toxicol. Sci. 60,
440 44–55. https://doi.org/10.1093/toxsci/60.1.44

441 California Natural Resources Agency, n.d. Periodic Groundwater Level Measurements - Datasets
442 - California Natural Resources Agency Open Data [WWW Document]. URL
443 https://data.cnra.ca.gov/dataset/periodic-groundwater-level-measurements (accessed
444 5.6.21).

445 California State Water Resources Control Board, 2020 GAMA Groundwater [WWW
446 Document]. Groundw. Ambient Monit. URL
447 https://gamagroundwater.waterboards.ca.gov/gama/gamamap/public/Default.asp (accessed
448 4.10.21).

449 Carle, D., 2015. Introduction to Water in California. University of California Press.

450 Conder, J.M., Hoke, R.A., De Wolf, W., Russell, M.H., Buck, R.C., 2008. Are PFCAs
451 bioaccumulative? A critical review and comparison with regulatory criteria and persistent
452 lipophilic compounds. Environ. Sci. Technol. https://doi.org/10.1021/es070895g

453 Crone, B.C., Speth, T.F., Wahman, D.G., Smith, S.J., Abulikemu, G., Kleiner, E.J., Pressman,
454 J.G., 2019. Occurrence of per- and polyfluoroalkyl substances (PFAS) in source water and
455 their treatment in drinking water. Crit. Rev. Environ. Sci. Technol. 49, 2359–2396.
456 https://doi.org/10.1080/10643389.2019.1614848

457 De Silva, A.O., Armitage, J.M., Bruton, T.A., Dassuncao, C., Heiger-Bernays, W., Hu, X.C.,
458 Kärrman, A., Kelly, B., Ng, C., Robuck, A., Sun, M., Webster, T.F., Sunderland, E.M.,
459 2021. PFAS Exposure Pathways for Humans and Wildlife: A Synthesis of Current
460 Knowledge and Key Gaps in Understanding. Environ. Toxicol. Chem.
461 https://doi.org/10.1002/etc.4935

462 Dodder, N.G., Maruya, K.A., Lee Ferguson, P., Grace, R., Klosterhaus, S., La Guardia, M.J.,
463 Lauenstein, G.G., Ramirez, J., 2014. Occurrence of contaminants of emerging concern in
464 mussels (Mytilus spp.) along the California coast and the influence of land use, storm water
465 discharge, and treated wastewater effluent. Mar. Pollut. Bull. 81, 340–346.
466 https://doi.org/10.1016/j.marpolbul.2013.06.041

467 Domingo, J.L., Nadal, M., 2019. Human exposure to per- and polyfluoroalkyl substances (PFAS)
468 through drinking water: A review of the recent scientific literature. Environ. Res.
469 https://doi.org/10.1016/j.envres.2019.108648

470 Douglas, G.S., Emsbo-Mattingly, S.D., Stout, S.A., Uhler, A.D., McCarthy, K.J., 2007.
471 Chemical fingerprinting methods, in: Introduction to Environmental Forensics. Elsevier
472 Inc., pp. 311–454. https://doi.org/10.1016/B978-012369522-2/50010-5

473 Elevation Point Query Service [WWW Document], n.d. URL https://nationalmap.gov/epqs/

(accessed 5.5.21).

Ericson, I., Nadal, M., Van Bavel, B., Lindström, G., Domingo, J.L., 2008. Levels of perfluorochemicals in water samples from Catalonia, Spain: Is drinking water a significant contribution to human exposure?, in: Environmental Science and Pollution Research. Springer, pp. 614–619. https://doi.org/10.1007/s11356-008-0040-1

Fasano, W.J., Carpenter, S.C., Gannon, S.A., Snow, T.A., Stadler, J.C., Kennedy, G.L., Buck, R.C., Korzeniowski, S.H., Hinderliter, P.M., Kemper, R.A., 2006. Absorption, distribution, metabolism, and elimination of 8-2 fluorotelomer alcohol in the rat. Toxicol. Sci. 91, 341–355. https://doi.org/10.1093/toxsci/kfj160

Fischer, G., Nachtergaele, F., Prieler, S., van Velthuizen, H.., Verelst, L., Wiberg, D., 2008. Global Agro-ecological Zones Assessment for Agriculture (GAEZ 2008). Laxenburg, Austria and Rome, Italy.

Frömel, T., Knepper, T.P., 2010. Biodegradation of fluorinated alkyl substances. Rev. Environ. Contam. Toxicol. 208, 161–177. https://doi.org/10.1007/978-1-4419-6880-7_3

Giesy, J.P., Kannan, K., 2001. Global distribution of perfluorooctane sulfonate in wildlife. Environ. Sci. Technol. 35, 1339–1342. https://doi.org/10.1021/es001834k

Houtz, E., Wang, M., Park, J.S., 2018. Identification and Fate of Aqueous Film Forming Foam Derived Per- and Polyfluoroalkyl Substances in a Wastewater Treatment Plant. Environ. Sci. Technol. 52, 13212–13221. https://doi.org/10.1021/acs.est.8b04028

Houtz, E.F., Higgins, C.P., Field, J.A., Sedlak, D.L., 2013. Persistence of perfluoroalkyl acid

precursors in AFFF-impacted groundwater and soil. Environ. Sci. Technol. 47, 8187–8195. https://doi.org/10.1021/es4018877

Houtz, E.F., Sedlak, D.L., 2012. Oxidative conversion as a means of detecting precursors to perfluoroalkyl acids in urban runoff. Environ. Sci. Technol. 46, 9342–9349. https://doi.org/10.1021/es302274g

Hu, X.C., Andrews, D.Q., Lindstrom, A.B., Bruton, T.A., Schaider, L.A., Grandjean, P., Lohmann, R., Carignan, C.C., Blum, A., Balan, S.A., Higgins, C.P., Sunderland, E.M., 2016. Detection of Poly- and Perfluoroalkyl Substances (PFASs) in U.S. Drinking Water Linked to Industrial Sites, Military Fire Training Areas, and Wastewater Treatment Plants. Environ. Sci. Technol. Lett. 3, 344–350. https://doi.org/10.1021/acs.estlett.6b00260

Hurley, S., Houtz, E., Goldberg, D., Wang, M., Park, J.S., Nelson, D.O., Reynolds, P., Bernstein, L., Anton-Culver, H., Horn-Ross, P., Petreas, M., 2016. Preliminary associations between the detection of perfluoroalkyl acids (PFAAs) in drinking water and serum concentrations in a sample of California women. Environ. Sci. Technol. Lett. 3, 264–269. https://doi.org/10.1021/acs.estlett.6b00154

Kannan, K., Corsolini, S., Falandysz, J., Fillmann, G., Kumar, K.S., Loganathan, B.G., Mohd, M.A., Olivero, J., Van Wouwe, N., Yang, J.H., Aldous, K.M., 2004. Perfluorooctanesulfonate and related fluorochemicals in human blood from several countries. Environ. Sci. Technol. 38, 4489–4495. https://doi.org/10.1021/es0493446

Kibbey, T.C.G., Jabrzemski, R., O'Carroll, D.M., 2020. Supervised machine learning for source allocation of per- and polyfluoroalkyl substances (PFAS) in environmental samples.

515 Chemosphere 252, 126593. https://doi.org/10.1016/j.chemosphere.2020.126593

516 Kim, K., Bennett, D.H., Calafat, A.M., Hertz-Picciotto, I., Shin, H.M., 2020. Temporal trends
517 and determinants of serum concentrations of per- and polyfluoroalkyl substances among
518 Northern California mothers with a young child, 2009–2016. Environ. Res. 186, 109491.
519 https://doi.org/10.1016/j.envres.2020.109491

520 Le, S.T., Kibbey, T.C.G., Weber, K.P., Glamore, W.C., O'Carroll, D.M., 2021. A group-
521 contribution model for predicting the physicochemical behavior of PFAS components for
522 understanding environmental fate. Sci. Total Environ. 764, 142882.
523 https://doi.org/10.1016/j.scitotenv.2020.142882

524 Lewis, R.C., Johns, L.E., Meeker, J.D., 2015. Serum biomarkers of exposure to perfluoroalkyl
525 substances in relation to serum testosterone and measures of thyroid function among adults
526 and adolescents from NHANES 2011–2012. Int. J. Environ. Res. Public Health 12, 6098–
527 6114. https://doi.org/10.3390/ijerph120606098

528 Maantay, J., 2002. Zoning law, health, and environmental justice: What's the connection?, in:
529 Journal of Law, Medicine and Ethics. Blackwell Publishing Inc., pp. 572–593.
530 https://doi.org/10.1111/j.1748-720X.2002.tb00427.x

531 Martin, J.W., Ellis, D.A., Mabury, S.A., Hurley, M.D., Wallington, T.J., 2006. Atmospheric
532 Chemistry of Perfluoroalkanesulfonamides: Kinetic and Product Studies of the OH Radical
533 and Cl Atom Initiated Oxidation of *N* -Ethyl Perfluorobutanesulfonamide. Environ. Sci.
534 Technol. 40, 864–872. https://doi.org/10.1021/es051362f

535 Martin, J.W., Mabury, S.A., O'Brien, P.J., 2005. Metabolic products and pathways of

fluorotelomer alcohols in isolated rat hepatocytes. Chem. Biol. Interact. 155, 165–180. https://doi.org/10.1016/j.cbi.2005.06.007

Mohai, P., Pellow, D., Roberts, J.T., 2009. Environmental Justice. Annu. Rev. Environ. Resour. 34, 405–430. https://doi.org/10.1146/annurev-environ-082508-094348

Mohai, P., Saha, R., 2015. Which came first, people or pollution? A review of theory and evidence from longitudinal environmental justice studies. Environ. Res. Lett. 10, 125011. https://doi.org/10.1088/1748-9326/10/12/125011

Parsons, J.R., Sáez, M., Dolfing, J., de Voogt, P., 2008. Biodegradation of perfluorinated compounds. Rev. Environ. Contam. Toxicol. 196, 53–71. https://doi.org/10.1007/978-0-387-78444-1_2

Plumlee, M.H., Kennedy/Jenks Consultants, Gurr, C.J., CDM Smith, Reinhard, M., 2011. Attenuation of Emerging Contaminants in Streams Augmented with Recycled Water | WateReuse Association.

Plumlee, M.H., Larabee, J., Reinhard, M., 2008. Perfluorochemicals in water reuse. Chemosphere 72, 1541–1547. https://doi.org/10.1016/j.chemosphere.2008.04.057

Prevedouros, K., Cousins, I.T., Buck, R.C., Korzeniowski, S.H., 2006. Sources, fate and transport of perfluorocarboxylates. Environ. Sci. Technol. https://doi.org/10.1021/es0512475

Rayne, S., Forest, K., 2009. Perfluoroalkyl sulfonic and carboxylic acids: A critical review of physicochemical properties, levels and patterns in waters and wastewaters, and treatment

556 methods. J. Environ. Sci. Heal. - Part A Toxic/Hazardous Subst. Environ. Eng.
557 https://doi.org/10.1080/10934520903139811

558 Sengupta, A., Lyons, J.M., Smith, D.J., Drewes, J.E., Snyder, S.A., Heil, A., Maruya, K.A.,
559 2014. The occurrence and fate of chemicals of emerging concern in coastal urban rivers
560 receiving discharge of treated municipal wastewater effluent. Environ. Toxicol. Chem. 33,
561 350–358. https://doi.org/10.1002/etc.2457

562 Sjogren, P., Montse, R., Lampa, E., Salihovic, S., van Bavel, B., Lind, L., Lind, P.M., 2016.
563 Circulating levels of perfluoroalkyl substances are associated with dietary patterns - A cross
564 sectional study in elderly Swedish men and women. Environ. Res. 150, 59–65.
565 https://doi.org/10.1016/j.envres.2016.05.016

566 State Water Resources Control Board, 2020. California State Water Resources Control Board.

567 US EPA, O., 2015. Occurrence Data for the Unregulated Contaminant Monitoring Rule.

568 Vestergren, R., Cousins, I.T., 2009. Tracking the pathways of human exposure to
569 perfluorocarboxylates. Environ. Sci. Technol. https://doi.org/10.1021/es900228k

570 Wager, S., Hastie, T., Efron, B., 2014. Confidence Intervals for Random Forests: The Jackknife
571 and the Infinitesimal Jackknife. J. Mach. Learn. Res. 15, 1625–1651.

572 Wang, Z., Boucher, J.M., Scheringer, M., Cousins, I.T., Hungerbühler, K., 2017. Toward a
573 Comprehensive Global Emission Inventory of C4-C10 Perfluoroalkanesulfonic Acids
574 (PFSAs) and Related Precursors: Focus on the Life Cycle of C8-Based Products and
575 Ongoing Industrial Transition. Environ. Sci. Technol. 51, 4482–4493.

https://doi.org/10.1021/acs.est.6b06191

Xu, Y., Jurkovic-Mlakar, S., Li, Y., Wahlberg, K., Scott, K., Pineda, D., Lindh, C.H., Jakobsson, K., Engström, K., 2020. Association between serum concentrations of perfluoroalkyl substances (PFAS) and expression of serum microRNAs in a cohort highly exposed to PFAS from drinking water. Environ. Int. 136, 105446. https://doi.org/10.1016/j.envint.2019.105446

Young, C.J., Mabury, S.A., 2010. Atmospheric perfluorinated acid precursors: Chemistry, occurrence, and impacts. Rev. Environ. Contam. Toxicol. 208, 1–109. https://doi.org/10.1007/978-1-4419-6880-7_1

Zhang, Y., Schaap, M.G., Zha, Y., 2018. A High-Resolution Global Map of Soil Hydraulic Properties Produced by a Hierarchical Parameterization of a Physically Based Water Retention Model. Water Resour. Res. 54, 9774–9790. https://doi.org/10.1029/2018WR023539